# Impact-Modified Polylactide–Calcium Sulfate Composites: Structure and Properties

**Miroslaw Pluta,[1] Marius Murariu,[2] Anne-Laure Dechief,[2] Leila Bonnaud,[2] Andrzej Galeski,[3] Philippe Dubois[2]**

[1]*Department of Polymer Structure, Centre of Molecular and Macromolecular Studies, Polish Academy of Sciences, Sienkiewicza 112, 90-363 Lodz, Poland*
[2]*Centre of Innovation and Research in Materials & Polymers (CIRMAP), Laboratory of Polymeric and Composite Materials (LPCM), University of Mons UMONS & Materia Nova Research Center, Place du Parc 20, 7000 Mons, Belgium*
[3]*Department of Polymer Physics, Centre of Molecular and Macromolecular Studies, Polish Academy of Sciences, Sienkiewicza 112, 90-363 Lodz, Poland*

Received 30 November 2011; accepted 30 November 2011
DOI 10.1002/app.36562
Published online in Wiley Online Library (wileyonlinelibrary.com).

**ABSTRACT:** The objective of the study is the preparation and comprehensive characterization of novel high performance polylactide (PLA)-based composites designed with specific impact properties. Highly filled composites were obtained by melt-blending PLA and 40 wt % anhydrite II (AII) microfiller, the dehydrated form of calcium sulfate hemihydrate, a by-product having as origin the lactic acid (LA) fabrication process. The toughness of PLA–AII composites was improved by addition of a selected impact modifier (IM) based on ethylene–acrylate copolymer (Biomax® Strong 100, noted BS). PLA–AII composites containing (10 wt %) BS were prepared using two procedures: (1) the direct melt blending of all components in a single step and (2) the previously coating of AII by BS, followed by mixing of coated filler with PLA. These approaches were carried out to modify the phase structure and to determine their influence on the final composite properties. As reference samples, PLA and PLA–BS blends were accounted. The miscibility and phase morphology (differential scanning calorimetry and scanning electron microscopy), thermal stability (thermogravimetric analysis), and thermomechanical properties (DMTA, tensile, and impact tests) were investigated to explain the toughening mechanism in the BS-modified composites. Noticeable, an attractive threefold increase of impact strength with respect to the composite without modifier and remarkable thermomechanical performances were assessed. The composite obtained using BS-coated AII showed better properties (e.g., impact strength of 5.4 kJ/m$^2$), improvements ascribed to the good filler dispersion and effective modification of interfacial regions (PLA–filler) by the BS-layer. © 2012 Wiley Periodicals, Inc. J Appl Polym Sci 000: 000–000, 2012

**Key words:** poly(lactic acid); calcium sulfate anhydrite; impact modifier; ethylene copolymer; mechanical properties

## INTRODUCTION

Over the past two decades, biodegradable polymers prepared from renewable resources have attracted great attention worldwide from both academic and industrial points of view. On the market of biodegradable polymers, polylactide (PLA) is undoubtedly one of the most promising candidates considered for further intensive industrial developments; it is not only biodegradable but also produced from renewable resources, like sugar beets or corn starch including their production wastes and excess.[1–3] PLA is currently receiving considerable attention for conventional applications such as packaging materials, textile fibre production and more recently, as composites for (semi)durable applications: electronic and electrical devices, mechanical and automotive parts, etc. Growing global environmental and social concern, the high rate of depletion of petroleum resources and new environmental regulations, are only some factors that have forced the search for new polymer materials compatible with the environment.[4]

In response to the demand for extending PLA applications range, while reducing its production cost, it has been recently demonstrated by some of us that commercially available PLA can be effectively melt blended with previously dehydrated gypsum [so called $CaSO_4$ anhydrite II (AII), details

*Correspondence to:* M. Pluta (mpluta@cbmm.lodz.pl).
Contract grant sponsors: CMMS PAS (Poland), Wallonia Region, Nord-Pas de Calais Region and European Commission for financial support in the frame of INTERREG projects: MABIOLAC and NANOLAC, European Commission and Région Wallonne FEDER program (Materia Nova) and OPTI$^2$MAT program of excellence, The Interuniversity Attraction Pole program of the Belgian Federal Science Policy Office (PAI 6/27) and by FNRS-FRFC.

**TABLE I**
**Innovative PLA–$CaSO_4$ (AII Form) Composites Obtained by Valorization of $CaSO_4$ By-Product From LA Fabrication Process**

| Composite | Principal characteristics | Potential utilization |
|---|---|---|
| PLA–$CaSO_4$ (AII) | Rigidity (high modulus), good tensile strength and thermal stability, barrier proprieties[7–10] | Biodegradable rigid packaging, engineering applications |
| PLA–AII–plasticizers | Improved toughness, cold crystallization properties, low glass transition temperature[12] | Packaging and applications requiring impact strength |
| PLA–AII–clays | Rigidity and thermal stability, increased time to ignition and low heat release rate, anti-dripping properties[3,13,14] | Rigid packaging, technical utilizations requiring specific fire retardancy |
| PLA–AII–halogen-free flame additives | Advanced flame-retardant properties, i.e., V0 rating (UL 94V test) obtained by co-addition of AII and selected halogen-free flame retardants[3] | Engineering applications requiring V0 classification such as electronic devices (e.g., housings of notebook computers) |

in Experimental Section], a by-product directly issued from lactic acid (LA) fabrication process.[5–9] These two products (PLA and AII) from the same source as origin can lead by melt mixing to polymer composites characterized by remarkable thermomechanical performances (thermal stability, rigidity, tensile strength, etc.[7–9]) and barrier properties[10] ascribed to excellent filler dispersion and good interface properties between the polymer matrix and microfiller.[7,11] Moreover, like for other mineral-filled polymers (PA, PET, PBT, etc.), addition of a third component[3,12–14] into PLA–AII compositions, i.e., plasticizers, clays, flame retardants, etc., has been considered to obtain new PLA grades with specific end-use performances (Table I).

Unfortunately, at filler amount higher than 20% (by weight), the filled composites are characterized by low impact strength properties.[7] Because for some potential applications, these composites do not have the required impact resistance, they need to be impact modified to fulfil the industry requirements. Addition of selected plasticizers, i.e., a general approach used to increase the impact strength of polymers, presents some drawbacks such as the decrease of tensile strength properties and of glass transition temperature ($T_g$). The thermal stability of plasticized PLA could also decrease due to the volatility/amount of some plasticizers that have been incorporated into the polyester matrix.[12]

Another important option that can be followed for increasing impact strength is represented by addition into PLA of selected impact modifiers (IMs).[15–21] Among the different commercially available IMs shown for improving PLA toughness, some specific ethylene copolymers (e.g., Biomax® Strong 100 – DuPont, noted herein BS) have been recently reported.[20,21]

The main goal of this contribution is to present some of the last results obtained in the investigation of the phase structure of highly filled (40% AII) PLA composites impact modified with BS and then, the correlation with the thermal and mechanical properties, to allow for a better understanding of the factors determining the effective impact improvement. For this purpose, to modify the interface properties between the polymer matrix and the dispersed phases (AII and BS), two techniques of dispersion have been considered: (1) the direct dosing of all components (PLA, AII and BS) during melt blending and (2) the previous coating of the microfiller (AII) by the IM (BS), step followed by melt mixing with PLA. The samples were characterized by using several experimental techniques to obtain complementary information about the phase structure (morphology) and its influence on the mechanical properties acquired under different deformation modes. Structural peculiarities, like dispersion of AII and BS into PLA matrix and the interface features between the components including the deformation behavior, were analyzed by scanning electron microscopy (SEM) on various samples exposed in cryofracture conditions, upon deformation in tensile test, as well as for the surfaces revealed by microtoming at ambient temperature. The thermal properties were determined using differential scanning calorimetry (DSC) and thermogravimetric analysis (TGA). Subsequently, the mechanical properties of the samples were characterized by different techniques [dynamic mechanical thermal analysis (DMTA), tensile, and impact testing], and these data were analyzed and correlated with the sample composition and the phase structure.

## EXPERIMENTAL

### Materials

PLA, number average molar mass = 74,500, polydispersity index 2.1, residual monomer content = 0.18%, D-isomer content = 4.3%, melt flow index (190°C, 2.16 kg) = 6.61 g/10 min, and density = 1.25 g/cm$^3$) was supplied by Galactic s.a. under the trade name Galastic. Calcium sulfate hemihydrate ($CaSO_4$

**TABLE II**
**Compositions and Codification of Samples**

| Entry | Sample composition (wt %) | *Codification of samples* |
|---|---|---|
| 1 | PLA | PLA |
| 2 | Biomax® Strong 100 | BS |
| 3 | PLA–40% AII | PLA–AII |
| 4 | PLA–10% BS | PLA–BS |
| 5 | PLA–40% AII–10% BS | PLA–AII–BS |
| 6 | PLA–40% AII–(c-10% BS)[a] | PLA–$AII_{cBS}$ |

[a] AII filler previously coated by BS; the AII/BS weight ratio = 4/1.

× 0.5 $H_2O$) with mean particle diameter ($d_{50}$) of 9 μm provided by Galactic s.a., a by-product issued from LA fabrication process, was used as filler after previous transformation into stable β-calcium sulfate AII by drying at 500°C.[7] An ethylene–acrylate copolymer, supplied by DuPont under the trade name BS, was selected to improve the impact strength and flexibility of PLA and PLA–AII composites. According to the supplier, typical characteristics of BS are as follows[17]: melting point: 72°C; glass transition temperature: −55°C; MFI (190°C/2.16kg): 12 g/10 min, tensile strength at break ≈ 5.2 MPa, and elongation at break = 950%.

## Melt-blending procedure and samples preparation

Before processing by melt blending, PLA was dried overnight at 80°C in a vacuum oven. To minimize the water content for melt blending with PLA, the BS and AII filler (coated or not by BS) were previously dried in an air circulating oven (at 50°C, overnight) and then, directly used for melt compounding. Starting from β-calcium sulfate hemihydrate, β-AII was obtained by dehydration for 1 h in a Nabertherm 3L furnace at 500°C as described elsewhere.[7]

Table II specifies the compositions and corresponding codification of the samples considered in this work. The PLA blends were obtained by melt compounding at a temperature of 200°C under moderate mixing (3 min premixing at 30 rpm, followed by mixing 3 min at 70 rpm) using a Brabender bench scale kneader equipped with cam blades. Two preparation methods of ternary composites have been considered. In the first one, all components (PLA, AII, and BS) were mixed together in one step. In the second one, the AII filler was previously surface coated with BS using the following procedure: a solution of 10% BS in THF was intensively mixed with AII for 3 h using a hot-plate magnetic-stirrer device (temperature of 40°C), step followed by drying to obtain a AII/BS blend in 4/1 weight ratio (as confirmed by TGA). Following this second approach, the coated filler, named herein $AII_{cBS}$, was used for melt mixing with PLA. For the sake of comparison the amount of BS was the same in both procedures. Neat PLA and PLA–BS blends were also prepared in similar conditions to obtain reference materials with comparable thermomechanical history. Throughout this paper, all percentages are given as wt %.

Samples for mechanical characterization were prepared by compression molding at 190°C using an Agila PE20 hydraulic press (low pressure for 240 s with three degassing cycles, followed by a high-pressure cycle at 150 bars for 150 s and cooling by tap water at 50 bars). Specimens for tensile and Izod impact testing were cut out from 3-mm thick plates by using a milling machine in accordance with ASTM D 638-02a norm (specimens type V) and ASTM D 256-A norm (specimens 60 × 10 × 3 $mm^3$), respectively. For DMTA, DSC, and TGA experiments film samples were used, i.e., about 0.8 mm thickness. All starting PLA-based samples were featured by an amorphous PLA matrix.

## Characterization

### Size exclusion chromatography

Molecular weight parameters (number average molar mass, $M_n$ and polydispersity index, $M_w/M_n$) of selected PLA materials were determined by size exclusion chromatography (SEC). The PLA materials were acquired from the unfilled PLA and from PLA specimens extracted from the composite systems. The procedure concerning the SEC measurements is detailed elsewhere.[7]

### Differential Scanning Calorimetry

Only the first DSC scan was considered to characterize the initial structure of the samples being the subject of analysis by different techniques. The thermal properties of the samples were investigated from 0 to 180°C with a rate of 3°C/min (under nitrogen atmosphere) using a DSC 2920 (TA Instruments). The thermal events of interest of PLA, i.e., the glass transition temperature ($T_g$), cold crystallization temperature ($T_c$), enthalpy of cold crystallization ($\Delta H_c$), melting temperature ($T_m$), and melting enthalpy ($\Delta H_m$) were determined. The thermal parameters of the neat BS were also determined using specimen prepared in similar mode like the PLA-based samples.

### Thermogravimetric analysis

TGA was performed under air by using a TGA Q50 (TA Instruments) with a heating ramp of 20°C/min from room temperature up to 600°C (platinum pan, 60 $cm^3$/min air flow rate).

### Mechanical testing measurements

Tensile tests were performed with a Lloyd LR 10K tensile bench in accordance to the ASTM D 638-02a

norm (speed rate = 1 mm/min, distance between grips = 25.4 mm). Notched impact strength (Izod mode) measurements were carried out by using a Ray-Ran 2500 pendulum impact tester and a Ray-Ran 1900 notching apparatus, in accordance to the ASTM D 256 norm (method A: 3.46 m/s impact speed with a 0.668 kg hammer). For tensile and impact tests, specimens were previously conditioned for at least 48 h at 20 (±1)°C under relative humidity of 45 ± 5% and the values were averaged over five measurements.

### Dynamic mechanical thermal analysis

Dynamic mechanical properties of all samples were measured with an MkIII DMTA apparatus (Rheometric Scientific, Epsom, UK) in a dual-cantiliver bending mode (deformation amplitude 32 μm, peak to peak). Samples in the form of strips 28 × 10 × 0.8 $mm^3$ were investigated. The dynamic storage and loss moduli, $E'$ and $E''$, respectively, were determined at a constant frequency of 1 Hz and heating rate of 2°C/min in the temperature range from −100 to 140°C for PLA-based samples, and up to +10°C for BS sample.

### Scanning electron microscopy

SEM was used for the characterization of fillers (AII and $AII_{cBS}$) and for investigation of the phase morphology of all considered samples, i.e., PLA, PLA–BS blend, PLA–AII, PLA–AII–BS and PLA–$AII_{cBS}$ composites. To acquire a comprehensive structural characterization (via SEM), different techniques for the preparation of the samples have been studied: (i) cryofracturing at liquid nitrogen temperature, (ii) fracturing at ambient temperature during tensile testing, and (iii) microtoming at room temperature PLA composites containing both AII and BS as dispersed phases. The analyzed surfaces were previously coated with a thin layer of gold in a sputtering process. A Jeol 5500 LV scanning electron microscope was used at various image magnifications and an accelerated voltage of 10 kV.

## RESULTS AND DISCUSSION

### Preliminary considerations

First, it is noteworthy reminding that the AII filler was obtained by specific dehydration of gypsum hemihydrate, a by-product issued from LA fabrication process. Therefore, it exhibits higher chemical purity (positive aspect for the preservation of PLA molecular weights) with respect to the anhydrite obtained using natural gypsum rock, which generally contains diverse impurities such as metallic ions (e.g., $Mg^{2+}$) able to accelerate PLA degradation. Furthermore, by considering the potential interest of PLA–AII composites for different applications (see Table I), it is believed that the mode of co-addition (AII and IM) can determine the impact properties of the resulting ternary composites. It is also important to note that due to its relatively high content of D isomer (4.3%), the investigated PLA grade is characterized by low crystallization ability. Moreover, for simplification and easier interpretation, all PLA-based samples were prepared in a similar manner, leading to an amorphous structure as overall morphology.

Regarding the modifications of PLA molecular parameters, usually, desired and beneficial effects obtained by addition of fillers and additives come along with some drawbacks such as an important drop of the molecular weights unfortunately leading to the loss of the mechanical properties. It is well-known that the melt processing has as effect the decrease of PLA molecular weight, even when this polyester is intensively dried or the processing is conducted under inert atmosphere, to limit polyester degradation by hydrolysis or by thermo-oxidation, respectively.[22,23] In this context, it was interesting to get some information on the molecular parameters of pristine PLA (as granules), PLA melt processed and PLA extracted from the studied compositions. On one hand, confirming the PLA degradation susceptibility, neat (unfilled) PLA showed some reduction by about 15% of $M_n$, i.e., from 74,500 as granules to about 64,000 after melt processing at 200°C (see Experimental Section) even in absence of any filler or additive. On the other hand, the addition of AII into PLA or co-addition of AII and BS did not lead to additional decrease of molecular weights with $M_n$ of PLA–AII and PLA–AII–BS determined at 63,000 and 64,000, respectively. At the same time, the polydispersity index ($M_w/M_n$) of melt-processed PLA and PLA extracted from the composite systems, shows only minor variations in the interval 2.0–2.2. This means that addition of AII and BS does not have additional influence on the decrease of $M_n$ during melt processing, which represents an essential information for the purpose of analysis and the discussion of the investigated physical properties. Accordingly, the physical properties can be correlated directly with sample composition and phase structure without consideration of the effects resulted from the slight differences in $M_n$.

The phase structure of the impact-modified composites was differentiated by application of two techniques of preparation, via (a) addition of AII and IM concurrently into PLA (PLA–AII–BS sample) and (b) the previous coating of AII by BS in the main goal of producing of a core–shell morphology in which the elastomeric phase (BS) encapsulates the

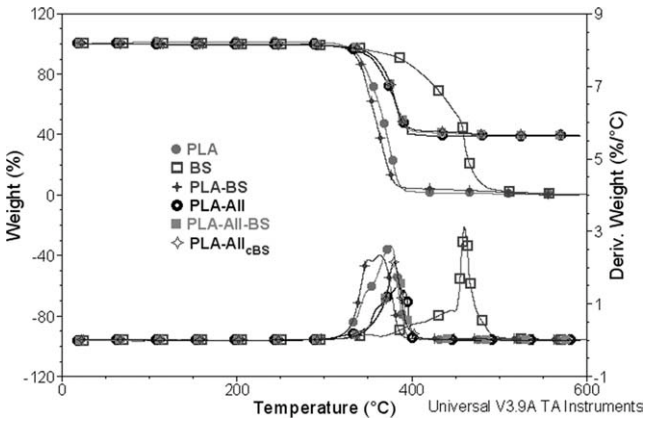


**Figure 1** TGA and DTG curves of the following samples: PLA, BS, PLA–BS, PLA–AII, PLA–AII–BS, and PLA–$AII_{cBS}$ (under air flow, 20°C/min).

microfiller (PLA–$AII_{cBS}$ sample). One can expect an influence of the elastomeric phase and the way of (co-)addition on the rheological behavior during melt blending, and subsequently on the structural features (e.g., dispersion, interactions, interface, etc.) that are determining the final properties of the composite.

### Thermal stability: TGA

Figure 1 shows TG and DTG curves recorded under air flow for PLA, BS, PLA–BS blend and ternary composites, i.e., PLA–AII–BS and PLA–$AII_{cBS}$. As the AII filler is stable in the considered temperature range,[7,8] the overall thermal stability of PLA–AII composite is significantly higher with respect to the unfilled PLA. BS is more resistant at thermal degradation than PLA, but in spite of this, the thermal stability of PLA–BS blend is not higher by comparing to the neat PLA.

This is ascribed to the relatively low loading of IM into PLA and to the specific morphology of the blend, the IM being dispersed as micrometric nodules into the polyester matrix.[20,21] Moreover, the presence of BS in both composites, i.e., PLA–AII–BS and PLA–$AII_{cBS}$, only slightly improves the thermal resistance with respect to the PLA–AII composite. In this context, it is of interest to mention that for these composites the 5% weight loss temperature ($T_{5\%}$) – which is often considered as the initial decomposition temperature, is above 345°C, whereas the temperature ascribed to the maximum rate of thermal degradation ($T_d$, from DTG) is above 380°C. Finally, by considering $T_{5\%}$ as reference parameter, the ternary composites containing BS show higher thermal stability with respect to PLA ($T_{5\%}$ = 334°C), and a tiny change is only recorded by comparing to PLA–AII ($T_{5\%}$ = 340°C), differences principally ascribed to the addition of filler and to somewhat better dispersion in presence of BS, respectively (see hereafter).

### Characterization of filler particles: SEM

Typical SEM micrographs of the neat AII and BS-coated AII ($AII_{cBS}$) are shown in Figure 2(a,b), respectively. Characteristic features of AII particles like their size, geometry and surface details can be clearly distinguished [Fig. 2(a)]. Majority of particles exhibit irregular shape with developed surface showing numerous hollows that are effective points of trapping for the molten PLA and BS during the melt compounding. Some particles with relatively flat surface are observed, too. The larger particles (up to about 10 μm) reveal features of aggregates composed of thinner lamellar units. Moreover, rod-like particles (about 0.2 μm width and 2.0 μm length) can be also occasionally observed.

In the case of $AII_{cBS}$, its surface details are completely hidden due to the coating of AII filler by BS [Fig. 2(b)]. The BS forms a layer encapsulating the filler particles as result of the pretreatment process (immersion and dispersion of AII in a solution of BS, followed by drying; see Experimental Section). Due to the specific preparation method, the $AII_{cBS}$

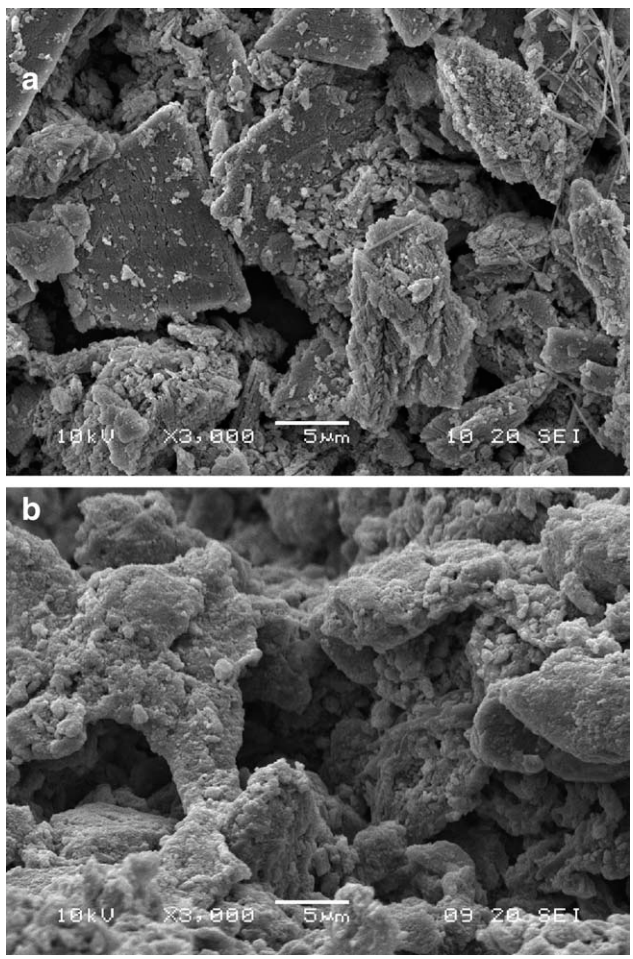


**Figure 2** Typical SEM micrographs of the neat AII (a) and $AII_{cBS}$ filler (b).

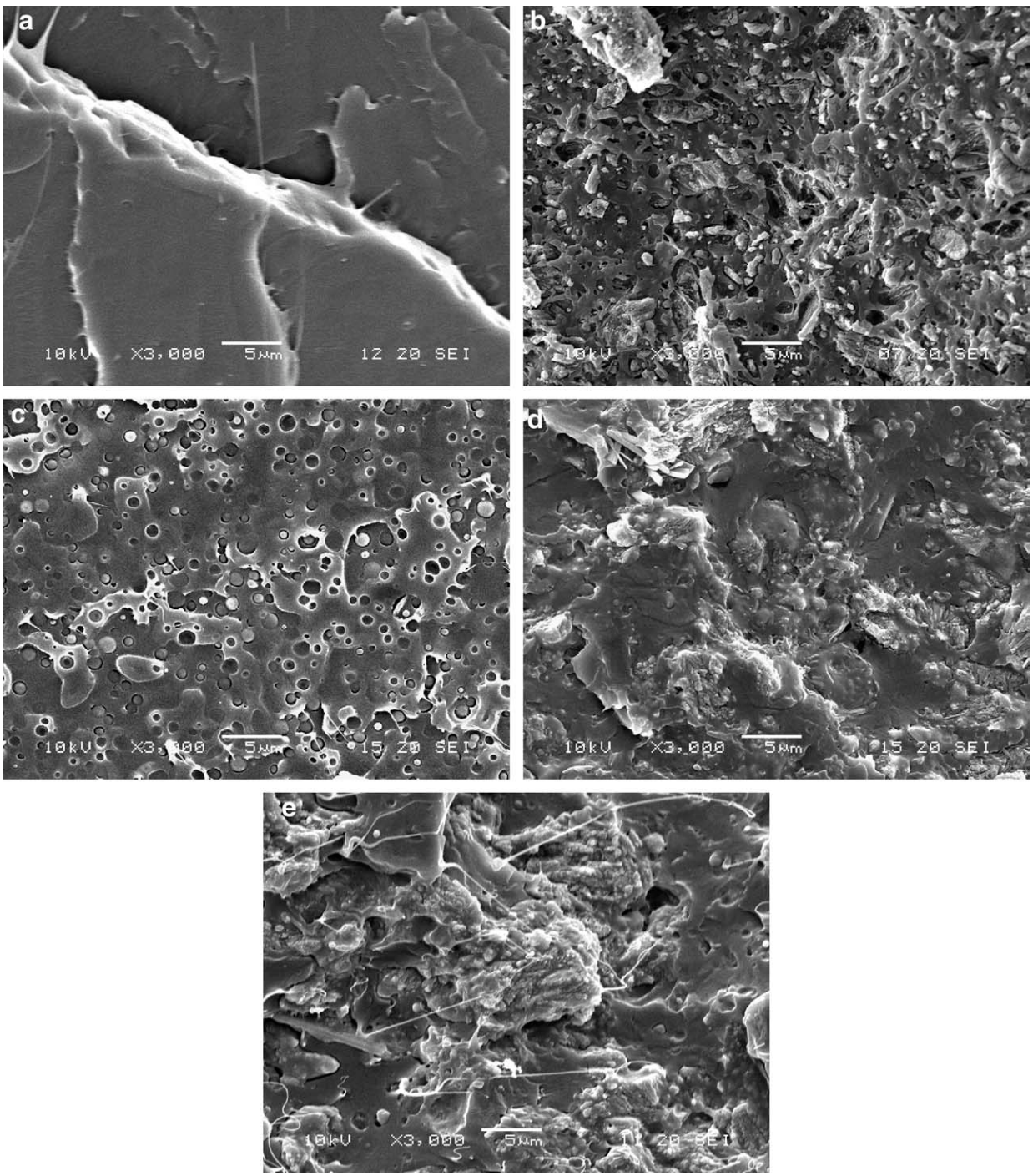


**Figure 3** SEM micrographs of different cryofractured surfaces: (a) neat PLA, (b) PLA–AII, (c) PLA–BS, (d) PLA–AII–BS, and (e) PLA–$AII_{cBS}$ (magnification 3000×, 10 kV).

particles are, more or less, stacked by the elastomeric BS phase.

### Phase morphology characterization: SEM

The phase morphology of the neat PLA and PLA-based samples were analyzed by SEM [Fig. 3(a–e)]. To acquire full information regarding the physical structure of the samples, surfaces prepared in different manner were analyzed: by cryofracturing (A), after microtoming at ambient temperature (B), and upon deformation during tensile testing (C).

(A) Figure 3(a–e) shows the cryofractured surfaces of neat PLA and PLA-based samples. Neat PLA shows a fairly smooth fracture surface, ascribed to a typical brittle failure, due to very little contribution of the plastic deformation [Fig. 3(a)]. Furthermore, the fractured surface of PLA–AII is more developed

showing the presence of "cavities" between PLA and AII, due to the debonding of the filler, and some number of hollows resulted from the removing of AII particles [Fig. 3(b)]. This surface illustrates relatively well dispersed AII particles, whereas some of them protrude from the polymer matrix. Their size is from the range 0.5–2 μm, whereas occasionally, voids or larger fragments of AII can be detected (4–10 μm). However, the debonding of filler particles from the matrix and cavitation formation by debonding have as consequence the absorption of energy during impact loading, which sometimes can explain the increase in impact strength (see Mechanical Characterization Section). The more detailed examination of the morphology of PLA–AII composite revealed the generation of cracking paths rather at the PLA–filler interface, without any evidence of cracking through the filler particles. This may suggest only weak adhesion between PLA and AII particles, aspects discussed more comprehensively in previous papers.[8,11] The strength of interfacial adhesion between PLA and AII partners estimated in a quantitative way is considered in the forthcoming paper.[24]

Regarding the PLA–BS blends, the SEM micrographs of the cryofractured surfaces show a relatively homogeneous distribution and dispersion of the IM in form of spherical domains with diameters of 0.5–1.5 μm [Fig. 3(c)]. This clearly indicates that PLA and BS components are immiscible, what is consistent with the results of additional analyses (see herein, DSC and DMTA). As results from Figure 3(c), the cracking paths go at the interface between BS and PLA (in cryogenic conditions) what is also evident in the pictures taken at higher magnification (not shown here). The phase morphologies, miscibilities and the different toughening mechanisms corresponding to the PLA–BS blends were assessed in a recent paper.[21] It is reasonable to suppose that the well dispersed elastomeric phase (BS) can have a dampening action in the brittle PLA matrix, capable to absorb impact energy and stop craze propagation.

Figure 3(d,e) illustrates the cryofractured surfaces of ternary composites, i.e., prepared by direct dosing of all components (PLA–AII–BS) and by melt-blending PLA with BS-coated AII particles (PLA–$AII_{cBS}$), respectively. As expected, their surfaces [Fig. 3(d,e)] are considerably different than those of PLA–AII composite [Fig. 3(b)] and PLA–BS blend [Fig. 3(c)]. On one side, the ternary systems reveal relatively flat surface of PLA matrix, without the characteristic hollows (voids) resulted from the removing of AII particles, which is typically observed in the case of PLA–AII composite. On the other side, separate BS microdomains quite well dispersed into PLA matrix, that are smaller and less numerous than in the PLA–BS blend [Fig. 3(c)] can be also observed. Following these observations, it is thought that during melt compounding of all components in a single step (PLA, AII, and BS), the BS modifier undergoes both dispersion into PLA matrix (forming separate micrometric nodules) as well as formation of a thin layer encapsulating partially or totally the surface irregularities of the AII filler. This modifies locally the interface in the boundary regions between PLA matrix and AII particles.

In turn, when PLA is blended with $AII_{cBS}$ [Fig. 3(e)], the thickness of the consistent initial BS layer present at the surface of microparticles is partially reduced, because some of its amount is also seen as dispersed phase (circular domains and fibrils) within the PLA matrix. The BS fraction forms inclusions in PLA matrix which are also smaller in dimension than those observed in the case of PLA–BS blend [Fig. 3(c)]. However, the BS layer thickness (and probably its continuity) is larger in the PLA–$AII_{cBS}$ than in PLA–AII–BS composite. This is reflected by the presence of plastically deformed BS fibrils in the boundary regions between PLA and AII within the PLA–$AII_{cBS}$ composite [Fig. 3(e)]. Such deformational effects are not observed in the case of PLA–AII–BS composite (as obtained in a single step), and this may suggest a poorer concentration of BS in the interfacial region PLA–microfiller.

(B) Additional SEM analyses were performed on the microtomed surfaces of the ternary composites. Microtoming was carried out deliberately at room temperature to have the BS modifier well above its $T_g$, whereas the PLA matrix is remaining still in the glassy state. In these conditions, the plastic deformation of the BS regions involved by the microtoming knife should be more developed and consequently more distinctly observed [Fig. 4(a,b)].

The surface of PLA–$AII_{cBS}$ [Fig. 4(b)] shows larger amount of plastically deformed BS modifier than those of PLA–AII–BS composite [Fig. 4(a)]. In fact, although the surface of PLA matrix is relatively flat, it is believed that the IM is principally localized in the boundary regions PLA–microfiller and it is oriented in the microtoming direction [Fig. 4(b)]. Contrarily, on the surface of PLA–AII–BS composite can be distinguished only tiny traces (of $\sim$ 1 μm) corresponding to the dispersed BS [Fig. 4(a)]. In addition, the surfaces prepared by microtoming reveal the internal structure of some larger AII particles showing a semigrain nature [Fig. 4(a)]. This particular filler can undergo further reduction in smaller particles or fragments, by intensive shearing during the melt compounding (e.g., in twin-screw extruders), as well as in the solid PLA matrix upon deformation in mechanical tests, when AII particles can behave as energy absorbing zones. Actually, it has been reported that composites containing phosphogypsum exhibit good ability to vibration damping.[25,26]

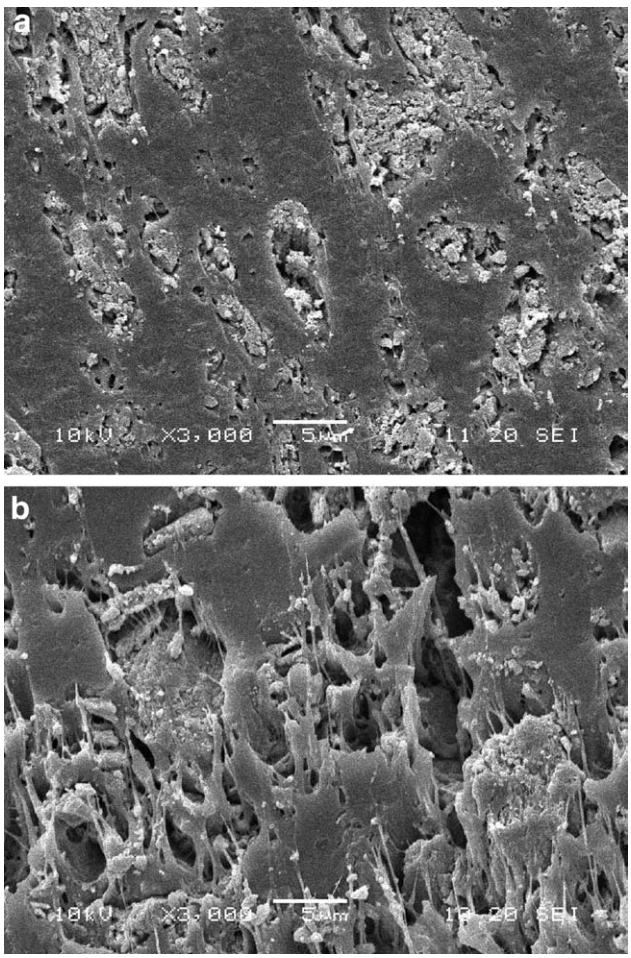


**Figure 4** SEM images (3000×) of the microtomed surfaces (at room temperature) of PLA–AII–BS (a) and PLA–$AII_{cBS}$ composites (b).

(C) Figure 5(a–e) shows selected SEM micrographs of the fractured surfaces revealed upon tensile testing at room temperature and lower deformation rate. In the case of neat PLA it can be seen a relatively flat and smooth surface, mainly attributed to a brittle failure [Fig. 5(a)]. However, the surfaces of the different PLA samples (PLA–AII, PLA–BS, and ternary composites) are primarily irregular due to the plastic deformation by mechanical shearing of PLA and BS phases [Fig. 5(b–e)].

In the case of PLA–AII composite, macrophase separation of the two components takes place; it is accompanied by the extensive plastic deformation of PLA matrix together with the (re)orientation of AII particles toward deformation direction [Fig. 5(b)]. Moreover, in the deformation process some cracking of larger AII particles composed of smaller lamellar units can also occur, as suggests Figure 5(d).

In the PLA–BS blends, both polymer components are plastically deformed [Fig. 5(c)]. PLA regions undergo ductile deformation forming elongated ligaments, whereas the BS phase is detected as circular inclusions closely fixed into PLA matrix (without observable separation of these both polymers). These BS inclusions are seemingly smaller than in the cryo-fractured surface of the same blend [compare Figs. 5(c) and 3(c)]. Actually, only the transversal size of stretched BS fibrils formed by shear yielding is observed.

Finally, the tensile fracture surfaces of the ternary composites are highly irregular, with numerous voids and elongated fibrils ascribed to the plastically deformed polymeric components (PLA and BS). This ductile deformation is due to shearing processes generated at boundaries of the three components (PLA, BS, and AII; Fig. 5(d,e)]. Interestingly enough, the filler particles are better revealed on the fracture surface of PLA–AII–BS [Fig. 5(d)] than in the PLA–$AII_{cBS}$ composite [Fig. 5(e)]. This can suggest rather higher adhesion of AII microfiller with the BS modifier than with the PLA matrix, and in this context, it is believed that the use of $AII_{cBS}$ characterized by a core(filler)–shell(elastomer) structure can lead to more beneficial proprieties.

### Thermal behavior: DSC

To favor the PLA cold crystallization and then, to correlate this process with the composition and the phase structure of PLA-based samples, a low heating rate (3°C/min) was used. At a faster heating scan, e.g., rate of 10°C/min, the crystallization events of the neat PLA (thus containing 4.3% D-LA isomer) were not observed.[20] To allow the characterization of the initial structure of the samples and then its reorganization upon heating in DSC apparatus, the thermal behavior was determined in the first DSC heating scan. The respective DSC thermograms are shown in Figure 6.

The glass transition temperatures ($T_g$) of the samples were of particular interest to determine whether the two polymeric components are (partially) miscible. From DSC data it comes out that the values of $T_g$ of PLA matrix are comparable (insignificant variations from 53.4 to 54.4°C) and moreover, it seems that this parameter ($T_g$) is not influenced by the composition of samples or preparation method. These results are also consistent with DMTA data (Viscoelastic Properties: DMTA Section, see below) that show a similar relation between the $T_g$ of samples (obtained from the peak of the loss modulus, $E''$). Therefore the presence of BS does not affect the $T_g$ of PLA confirming that PLA and BS are immiscible. This is consistent with the two-phase morphology clearly observed in the SEM micrographs of PLA–BS blend [Fig. 3(c)]. However, some possible changes of $T_g$ of PLA can be influenced by the superposed melting effect of the BS component (Fig. 6). This effect occurs in a wide temperature

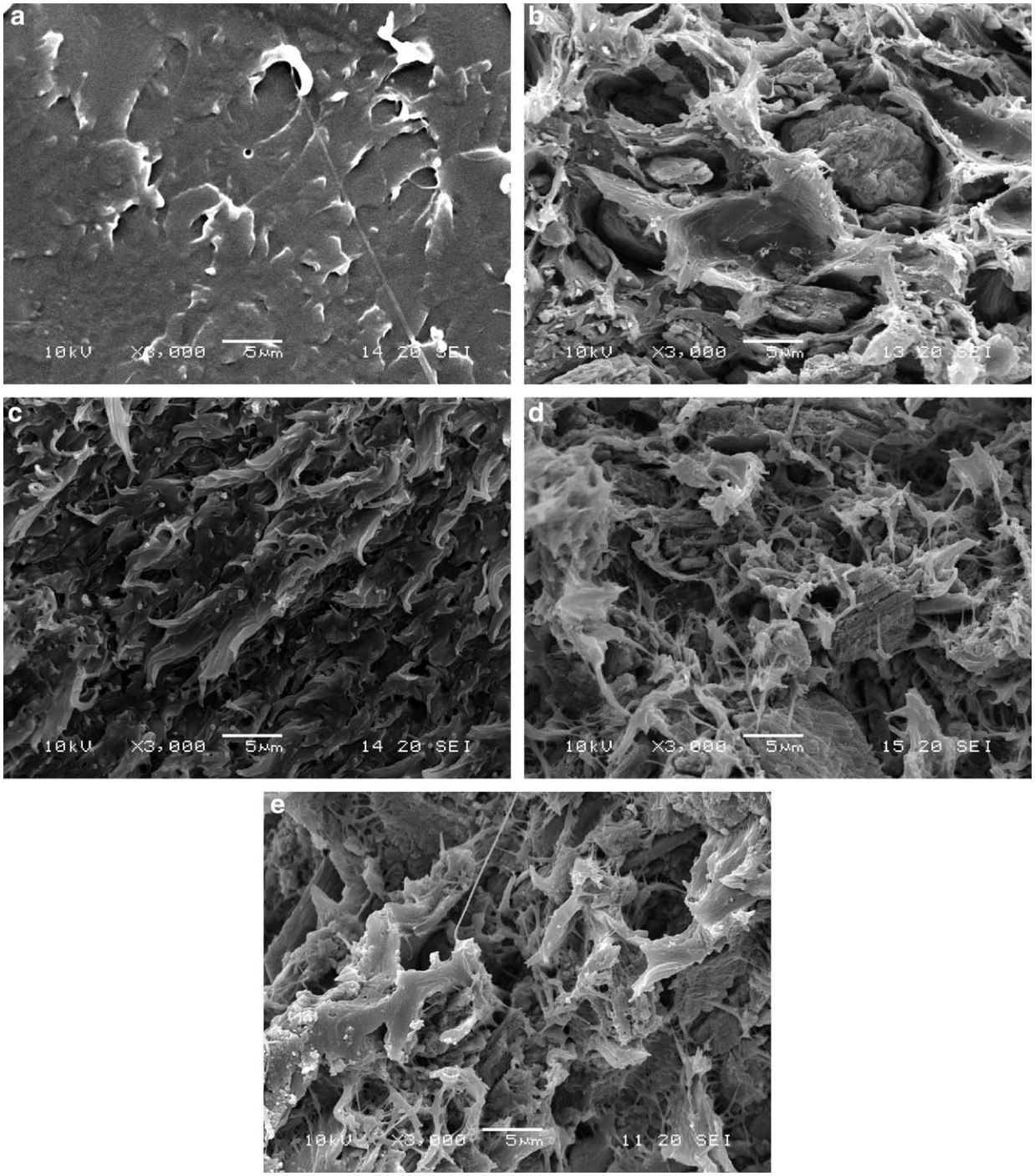


**Figure 5** SEM micrographs of the tensile fractured surfaces: (a) neat PLA, (b) PLA–AII, (c) PLA–BS, (d) PLA–AII–BS, and (e) PLA–AII$_{cBS}$.

range, from $\sim$ 20 to 80°C, as two broad overlapping endotherms (marked by inset in Fig. 6): their maximum are at $T_m \approx 39.4$°C and 72.0°C, whereas the total melting enthalpy value is $\Delta H_c = 39.1$ J/g. This means that in contrast to the PLA matrix, the BS copolymer is readily crystallizable. It is worth noting that amorphization of BS was not possible neither via the melt-quenching procedure, i.e., during the sample preparation, or during faster cooling in DSC apparatus with a ramp of −100°C/min down to −100°C. Furthermore, during this DSC cooling scan a distinct crystallization peak appeared around the temperature of 40°C, whereas in the subsequent reheating scan (10°C/min) the BS sample showed a $T_g$ around −46.6°C (these DSC cooling–heating thermograms are not shown here).

In turn, the initial structure of PLA in all PLA-based samples is amorphous as the corresponding

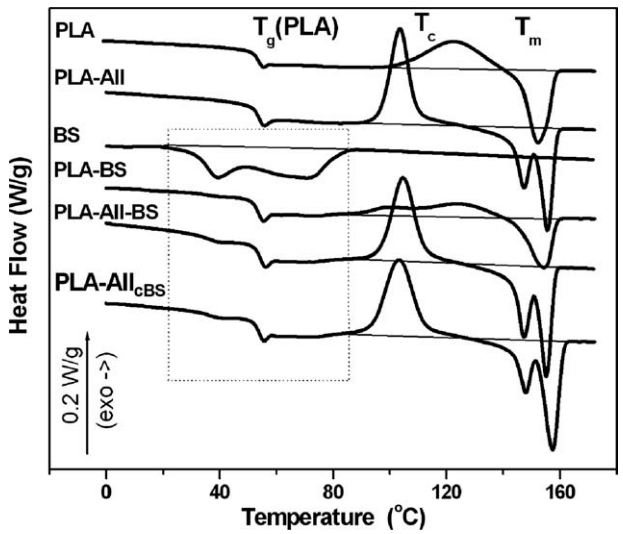


**Figure 6** DSC heating thermograms of the following samples: PLA, PLA–AII, BS, PLA–BS, PLA–AII–BS, and PLA–AII$_{cBS}$ (heating ramp of 3°C/min). (Except for the BS sample, the curves are related to the unit mass of PLA.)

enthalpies of the cold crystallization ($\Delta H_c$) and melting processes ($\Delta H_m$) are comparable. However, it is of interest to mention that the ability to crystallize of the PLA matrix is affected by the sample composition. The neat PLA shows a broad cold crystallization exotherm ($T_c$ = 122.5°C, $\Delta H_c$ = 19.5 J/g) and a single melting peak ($T_m$ = 152.2°C, $\Delta H_m$ = 20.5 J/g). For PLA–AII composite the cold crystallization process is shifted toward lower temperature and $\Delta H_c$ increased distinctly ($T_c$ = 103.5°C, $\Delta H_c$ = 28.7 J/g), whereas its melting becomes more complex showing double peaks ($T_m$ = 147.2 and 155.5°C, $\Delta H_m$ = 30.5 J/g). Ternary composites are characterized by similar DSC thermograms. Namely, the PLA–AII–BS composite is featured by $T_c$ = 104.6°C, $\Delta H_c$ = 31.0 J/g and $T_m$ = 147.2 and 155.0°C, $\Delta H_m$ = 31.7 J/g, whilst the PLA–AII$_{cBS}$ composite shows $T_c$ = 103.2°C, $\Delta H_c$ = 32.1 J/g and $T_m$ = 147.8 and 157.3°C, and $\Delta H_m$ =32.7 J/g.

Generally, one can observe that the AII filler enhances the cold crystallization ability of the PLA matrix (PLA–AII, PLA–AII–BS, and PLA–AII$_{cBS}$ samples). This effect can be explained by some nucleation activity of AII toward PLA (it exists also during PLA crystallization from the melt[8]). However, the PLA crystallites formed in the composites have different thermal stability as it is reflected by the double melting peaks (Fig. 6).

In contrast, the BS copolymer restrains the cold crystallization of the polyester matrix. This is particularly seen for the PLA–BS blend that exhibits less intense double exotherms ($T_c$ = 100.0 and 123.7°C, $\Delta H_c$ = 14.7 J/g and $T_m$ = 154.2, $\Delta H_m$ =14.7 J/g).

Interestingly, the DSC thermograms of BS-containing samples (PLA–BS, PLA–AII–BS, and PLA–AII$_{cBS}$) show a small endothermic effect around the temperature of 40°C: it coincides with the low-temperature endotherm of the neat BS sample and this indicates the semicrystalline state of the BS rubbery phase into the PLA matrix. To summarize, some thermal parameters issued from the discussion of DSC thermograms appeared to be sensitive to the sample composition. However, they do not revealed any characteristic features that could be ascribed to the difference of phase structure between the PLA–AII–BS and PLA–AII$_{cBS}$ composites. The same conclusion flows from the analysis of the DSC second heating scan (data not discussed here).

### Viscoelastic properties: DMTA

Figure 7(a) displays the storage modulus ($E'$) vs. temperature evolution for all investigated samples: the neat polymeric components (PLA and BS), their blend (PLA–BS), PLA–AII composite, as well as the ternary composites (PLA–AII–BS and PLA–AII$_{cBS}$). $E'$ decreases gradually with temperature showing faster decrease at about −45°C for neat BS and BS-containing samples (assigned to $T_g$ of BS). Then, a much more marked drop of the curve is observed at ca. 50°C for neat PLA and all PLA-based samples, which corresponds to $T_g$ of PLA (see Table III). Subsequently, the $E'$ shows some increase above ca. 90°C with a maximum depending on the specific composition of the investigated sample (this point is discussed in more detail below).

The analysis of $E'$ spectrum shows the distinct dependence between the sample composition and their phase structure. For example, AII reinforces PLA matrix as the $E'$ values of all AII-containing composites appear higher with respect to neat PLA and PLA–BS blend in the whole temperature range. Interestingly enough, the BS component in the glassy state, i.e., below its $T_g$, additionally reinforces both PLA–BS blend and ternary composites. This increase is slightly higher for PLA–AII$_{cBS}$ composite than in case of PLA–AII–BS, more likely as a result of (i) larger interfacial regions within the polymer matrix and (ii) thicker BS layer located in between PLA and AII microparticles in the former composite (assumption consistent with SEM observations). Such behavior should improve the interfacial adhesion between the individual components (PLA and AII, PLA and BS, AII and BS) allowing some more effective stress transfer at low deformations. In turn, at temperature above the $T_g$ of BS, all samples containing BS are characterized by a further decrease of $E'$ due to the glass-to-rubber transition of the BS component.

For simplification and easier interpretation, some selected values of $E'$ recorded at representative temperatures are given in Table III. It comes out that the

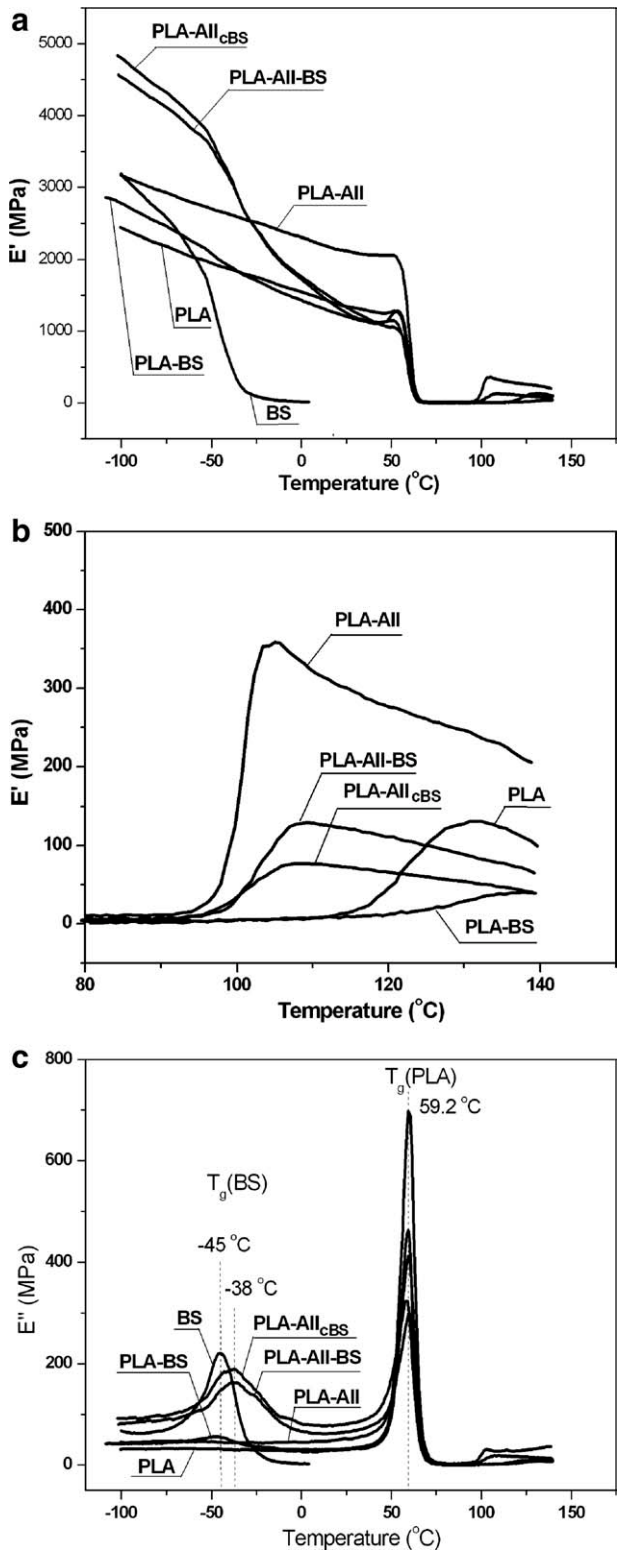


**Figure 7** (a) Temperature dependence of the storage modulus ($E'$) of the following samples: PLA, BS, PLA–AII, PLA–BS, PLA–AII–BS, and PLA–AII$_{cBS}$. (b) Changes in storage modulus ($E'$) in the cold crystallization temperature region for PLA and PLA-based samples (PLA–AII, PLA–BS, PLA–AII–BS, and PLA–AII$_{cBS}$). (c) Temperature dependence of the loss modulus ($E''$) of the following samples: PLA, BS, PLA–AII, PLA–BS, PLA–AII–BS, and PLA–AII$_{cBS}$.

mechanical properties ($E'$) of the considered samples show typical temperature dependence.

Figure 7(b) illustrates more precisely the evolution of $E'$ for PLA-based samples in the temperature range coinciding with the cold crystallization of PLA matrix, to show how this mechanical parameters are influenced by the composition and phase structure. Namely, the $E'$ values (for instance at 120°C) fulfill the following relation: $E'_{(\text{PLA-AII})} > E'_{(\text{PLA-ALL-BS})} \geq E'_{(\text{PLA-ALLcBS})} > E'_{(\text{PLA})} > E'_{(\text{PLA-BS})}$. At the same time the crystallinity development of the three composites (PLA–AII, PLA–AII–BS, and PLA–AII$_{cBS}$) in this region of temperature is more or less comparable (see the cold crystallization peaks, Fig. 6). This means that the crystallinity degree of the PLA matrix is one of the parameters that can influence the $E'$ value of these composites. The other factors are related to the properties of the BS modifier dispersed in the PLA matrix, and particularly to the BS phase located in the boundary regions between PLA and AII. This BS layer is already molten in the considered temperature range, therefore, it only insufficiently transfers stresses between PLA matrix and AII filler. This means that a thicker and more continuous BS layer will reduce more intensively the $E'$ value, what is actually consistent with the observed relation: $E'_{(\text{PLA-AII})} > E'_{(\text{PLA-ALL-BS})} > E'_{(\text{PLA-ALLcBS})}$.

Figure 7(c) illustrates the temperature dependence of the loss modulus ($E''$) for the different studied samples. For the neat PLA and PLA–AII composite only two peaks of $E''$ in the considered temperature range are observed, which can be respectively assigned to the glass–rubber transition of the polyester matrix ($T_{g(\text{PLA})} \approx 59.0$°C) and, the PLA cold crystallization process at higher temperature, i.e., above 80°C. The latter indicates clearly that the crystalline PLA zones further enhance the mechanical loss ($E''$). Like an illustration of the role of the interfacial regions between PLA and AII in the mechanical loss generation, one can observe also that the $E''$ values are higher for PLA–AII than PLA, particularly in the $T_{g(\text{PLA})}$ region.

In turn, all BS-containing samples, show a third peak at negative temperature, ascribed to the glass–rubber transition of the BS phase and indicating again the immiscibility between PLA and BS. $E''$ evolution shows a maximum at ≈−45°C ($T_{g(\text{BS})}$) for the PLA–BS blend, whereas interestingly, the maximum for the ternary composites appears with a larger intensity and at a higher temperature (−38.0°C). This effect directly indicates that the intensive mechanical loss is generated within the BS layer sandwiched between PLA and AII. Its magnitude is slightly higher for the PLA–AII$_{cBS}$ composite than PLA–AII–BS, difference could be again attributed to a thicker layer and to a more continuous BS phase in the former composite. The shift of the $T_{g(\text{BS})}$ by about 7°C toward higher temperature observed for the

**TABLE III**
**Comparison of $E'$ Values for the Samples as Recorded at Characteristic Temperatures**

| | Storage modulus ($E'$) (MPa) | | | |
|---|---|---|---|---|
| | Temperature | | | |
| Sample | −80°C below $T_{g(BS)}$, below $T_{g(PLA)}$ | 20°C above $T_{g(BS)}$, below $T_{g(PLA)}$ | 80°C above $T_{g(BS)}$ and $T_{m(BS)}$, above $T_{g(PLA)}$ | 120°C $T_{cc}$ region of PLA |
| BS | 2700 | – | – | – |
| PLA | 2230 | 1370 | 3.4 | 46 |
| PLA–AII | 2960 | 2140 | 10.5 | 276 |
| PLA–BS | 2520 | 1650 | 2.8 | 13 |
| PLA–AII–BS | 4210 | 1400 | 7.8 | 111 |
| PLA–$AII_{cBS}$ | 4400 | 1335 | 5.4 | 106 |

$T_{cc}$, cold crystallization temperature

BS-containing PLA–AII composites likely results from the stressed state of the BS layer between PLA and AII due to different thermal expansion coefficients of the composite components. This indicates the significance of the interface and transition regions (like BS layer) in the dissipation of the mechanical energy during periodical deformation.

Concerning the maximum of loss modulus ($E''$) of all BS-containing samples (PLA–BS, PLA–$AII_{cBS}$, and PLA–AII–BS) in the $T_{g(PLA)}$ region, it was observed that its height was more or less comparable, but somewhat lower and broader than the value recorded for neat PLA. Such an observation more likely results from the melting contribution of the BS component previously detected in DSC thermograms (Fig. 6). Accordingly, a more detailed analysis concerning the changes of $T_{g(PLA)}$ values is made rather difficult. It is worth pointing out that the evolution of $E''$ in the PLA cold crystallization region follows the relations established for $E'$.

## Tensile and impact properties

The dynamic mechanical analysis carried out in a large temperature interval was completed with the results of the tensile and impact testing performed under ambient conditions, thus in between $T_g$'s of BS and PLA.

In Table IV are shown the comparative mechanical properties of the neat PLA and PLA–AII composites containing or not BS (according to standard recommendations, PLA–BS was evaluated at higher speed of testing and in this context these results are not shown here).

Concerning the tensile properties, it is important to remind that it was reported by some of us that the rigidity (Young's modulus) of PLA–AII composites is systematically increasing with the increase in filler loading.[7] Moreover, as seen in Table IV, Young's modulus reaches about 2300 MPa by addition of 40% AII, value considerably higher with respect to unfilled PLA (1450 MPa). At the same time, the tensile strength decreased from about 65 MPa (neat PLA, Entry 1) to about 48 MPa for PLA–AII composite (40% AII), a value that remains sufficiently high in the perspective of further applications. These excellent tensile properties were accounted for to the good filler dispersion. In other context, addition of a rubber component into a polymeric matrix typically improves the toughness but can also lead to a decrease of tensile strength in correlation to the relative content in modifier. Indeed, addition of the BS modifier into PLA–AII composites leads to further modification of the mechanical properties. On one hand, as it comes out from the results shown in Table IV for the ternary composites containing BS (Entries 3 and 4), both Young's modulus and the tensile strength are decreased; this is as a consequence of the rubber behavior of the BS modifier and of its low mechanical strength (tensile strength $\approx$ 5 MPa, see Experimental Section) at the testing temperature. However, an interesting

**TABLE IV**
**Comparative Mechanical Properties of Neat PLA and of PLA–AII Composites Containing or Not BS as IM (Standard Deviations Are Given in Brackets)**

| Entry | Sample | Max. tensile strength (MPa) | Young's modulus (MPa) | Nominal strain at break (%)[a] | Impact strength-Izod ($kJ/m^2$) |
|---|---|---|---|---|---|
| 1 | PLA | 65 (± 2) | 1450 (± 150) | 9.3 (± 0.9) | 2.6 (± 0.2) |
| 2 | PLA–AII | 48 (± 2) | 2300 (± 100) | 3.3 (± 0.3) | 1.5 (± 0.7) |
| 3 | PLA–AII–BS | 22 (± 1) | 2000 (± 200) | 3.5 (± 0.3) | 3.6 (± 0.2) |
| 4 | PLA–$AII_{cBS}$ | 26 (± 1) | 1950 (± 50) | 5.1 (± 1.0) | 5.4 (± 0.7) |

[a] Distance between grips of 25.4 mm.

difference between the mechanical properties of these ternary composites can be distinguished. For PLA–AII$_{cBS}$ the tensile strength is higher (26 MPa) than for PLA–AII–BS composite prepared in a single step (max. tensile strength of 22 MPa), whereas Young's modulus is showing comparable values, 1950 MPa and 2000 MPa, respectively. These changes in the considered mechanical parameters reflect the differentiation of the phase structure observed by SEM. BS is present at different level at the PLA–AII interface and as microdomains spread into the polyester matrix, without excluding the influence on mechanical properties of additional factors such as a possible advanced dispersion of AII$_{cBS}$ into PLA matrix, or a supplementary fragmentation of AII particles along with the coating step by BS layer. One can assume that the direct addition of BS or its use for the coating of AII filler leads rather to the decrease of the strength of particle–particle and matrix–filler interactions, which will affect the tensile strength proprieties. The reported difference in the location of BS resulted from different compounding protocol are explained schematically in Figure 8.

On the other hand, as expected, for all composites representing heterogeneous systems the nominal strain at break is decreased in comparison with neat PLA, from about 9.3% (PLA) to 3.3–5.1% for the studied composites (Table IV). In contrast to neat PLA, the PLA–AII composite (Entry 2) undergoes the break at the lowest elongation (3.3%), whereas the addition of BS (rubber component) leads to different effects in the ternary composites. Although the PLA–AII–BS composite does not show any significant increase of the nominal strain at break (3.5%), the PLA–AII$_{cBS}$ composite containing BS-coated filler shows a higher value, i.e., 5.1%. This indicates that the BS layer present between PLA and AII contributes to the effective evolution of the plastic deformation processes in this composite, at least at local level. Moreover, these assumptions are consistent with the results of SEM investigations of the fractured surfaces of the PLA–AII$_{cBS}$ composite.

Concerning the impact resistance, it was shown[7] that by filling PLA with up to 20% AII, the PLA–AII composite exhibits somewhat increase of the impact resistance to about 3.1 kJ/m$^2$ (compared with 2.6 kJ/m$^2$, neat PLA). Furthermore, in relation to the toughness properties, it is of interest to remind that in some cases the rigid filler particles can improve the impact strength following a multistep toughening mechanism (stress concentration, debonding, shear yielding, etc.).[27] However, at higher filler content a distinct drop of the impact resistance occurred, as a typical feature of highly filled polymer composites, ascribed to the presence of more heterogeneous (mechanically weak) regions, e.g., remaining filler aggregates poorly dispersed within the matrix.

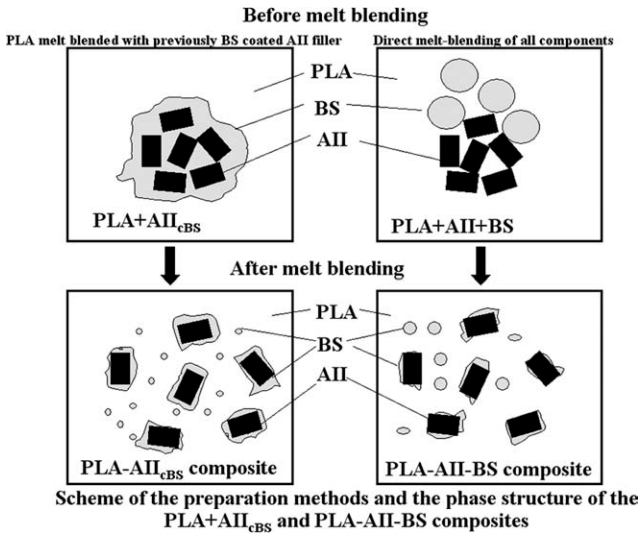


**Figure 8** Scheme of the preparation methods and the phase structure of the PLA + AII$_{cBS}$ and PLA–AII–BS composites.

Thus, it was interesting to determine the role of BS modifier on the impact resistance of the BS-containing PLA–AII composites featured by high content of AII filler (40%). First, it is important to remind that in the case of PLA–BS blends an effective improvement of toughness, irrespective to the nature of the PLA matrix (amorphous, crystalline) has been reported.[20,21] For example, addition of 10% BS into PLA leads to an increase of the impact strength from a value of 2.6 kJ/m$^2$ (neat PLA) to about 12.4 kJ/m$^2$.[20] It was generally observed in our SEM investigations (Phase Morphology Characterization: SEM Section), that in the blends with 10 wt % or more IM (BS), their fracture arose through crazing, IM fibrillation, crack bridging, debonding cavitation, and matrix shear yielding resulting in ductile behavior, these mechanisms being able to dissipate the energy involved in the impact fracture of toughened PLA.[21]

Assuming these possible mechanisms and corroborated with the investigation of morphology, as follows from Table IV, BS effectively acts as IM also for the BS-containing PLA–AII composites. Although for PLA–AII composite the impact strength is very low, i.e., 1.5 kJ/m$^2$ (and below neat PLA, 2.6 kJ/m$^2$), one notice a twofold increase for the PLA–AII–BS composition (3.6 kJ/m$^2$), and even a threefold increase for the PLA–AII$_{cBS}$ composite (5.4 kJ/m$^2$). The comparison of the last two results clearly indicates the significance of the phase structure in determining the toughness properties of the ternary composites at the high deformation rate applied during impact solicitation. Particularly, it is confirmed the role of the BS-layer between PLA matrix and AII filler, which improves distinctly the ability of this composite (PLA–AII$_{cBS}$) to dissipate the energy provided during impact loading. Knowing the $T_g$ of BS at

about −50°C, it can be assumed that the ternary composites can be tailored for application over a wider temperature region, below its $T_m$, including negative temperatures. Finally, as far as the mechanical properties are concerned, even that some parameters require further optimization (e.g., tensile strength), the addition of BS as third component into PLA–AII composites represents an interesting choice leading to favorable increases of the impact strength (better results using $AII_{cBS}$). This is ascribed to BS dispersion at micrometric level into PLA matrix and to its effects in the changing of interfacial properties, without excluding the influence of additional factors such as better filler dispersion and deagglomeration.

## CONCLUSIONS

The preparation and comprehensive investigation of PLA-based composites filled with high amount (40%) of $CaSO_4$ (AII form) and impact modified with 10% ethylene–acrylate copolymer (BS) have been carried out. AII filler was obtained by specific dehydration of gypsum by-product resulted from the LA fabrication process. BS was selected as IM to improve the toughness of highly filled PLA–AII composites taking into account two techniques of addition: (1) the direct melt blending of all components in a single step and (2) the previously coating of AII by BS, followed by melt-mixing PLA with the resulting $AII_{cBS}$. These two approaches allow for differentiating the phase structure of ternary composites and to evidence its role in determining the thermal and mechanical properties. It was shown that the presence of AII filler and/or BS did not negatively affect the PLA molecular parameters, whereas the overall thermal stability has been improved by co-addition of AII and BS (TGA). However, the additives modified the ability of PLA matrix to undergo cold crystallization process. Actually, AII particles proved to facilitate it, whereas BS copolymer restrained it. Moreover, the immiscibility of PLA and BS was evidenced by using several techniques of analysis such as SEM, DSC and DMTA.

The mechanical performances of the ternary composites were comparatively evaluated by tensile and impact testing. By comparison with the composite without IM (PLA–AII), the addition of BS led to the desired increase of the impact properties. Noticeable, the increase of impact strength was more important using BS-coated filler ($AII_{cBS}$, 5.4 kJ/m$^2$) than by direct mixing of all components (3.6 kJ/m$^2$). Corroborated with better tensile strength, these improvements, accordingly to the detailed SEM investigations and analyses of the viscoelastic spectra (including characteristic relaxation processes in DMTA), can be ascribed to the modification of the phase boundary regions between PLA matrix and AII filler by the incorporation of BS layer. Finally, by considering the thermomechanical properties and structural modifications, it is believed that the "core(filler)–shell(elastomer)" approach could disclose a practical interest in production of PLA composites designed with improved impact properties.

They also thank their partners for helpful discussions and all mentioned companies for supplying raw materials.

## References

1. Platt, D. Biodegradable polymers—market report. Smithers Rapra Limited, UK, Shawbury, Shrewsbury, Shropshire, 2006.
2. Drumright, R. E.; Gruber, P. R.; Henton, D. E. Adv Mater 2000, 12, 1841.
3. Dubois, Ph.; Murariu, M. JEC Compos Mag 2008, 45, 66.
4. Avella, M.; Buzarovska, A.; Errico, M. E.; Gentile, G.; Grozdanov, A. Polym Compos Mater 2009, 2, 911.
5. Narayanan, N.; Roychoudhury, P. K.; Srivastava, A. Electron J Biotechnol 2004, 7, 167.
6. Mecking, S. Angew Chem Int 2004, 43, 1078.
7. Murariu, M.; Da Silva Ferreira, A.; Degée, Ph.; Alexandre, M.; Dubois, Ph. Polymer 2007, 48, 2613.
8. Pluta, M.; Murariu, M.; Da Silva Ferreira, A.; Alexandre, M.; Galeski, A.; Dubois Ph. J Polym Sci Part B Polym Phys 2007, 45, 2770.
9. Pluta, M.; Murariu, M.; Alexandre, M.; Galeski, A.; Dubois, Ph. Polym Degrad Stabil 2008, 93, 925.
10. Gorrasi, G.; Vittoria, V.; Murariu, M.; Da Silva Ferreira, A.; Alexandre, M.; Dubois Ph. Biomacromolecules 2008, 9, 984.
11. Molnár, K.; Moczo, J.; Murariu, M.; Dubois, Ph.; Pukánszky, B. eXPRESS Polym Lett 2009, 3, 49.
12. Murariu, M.; Da Silva Ferreira, A.; Pluta, M.; Bonnaud, L.; Alexandre, M.; Dubois, Ph. Eur Polym J 2008, 44, 3842.
13. Murariu, M.; Bonnaud, L; Yoann, P.; Fontaine, G.; Bourbigot, S.; Dubois, Ph. Polym Degrad Stabil 2010, 95, 374.
14. Dubois, Ph.; Murariu, M.; Alexandre, M.; Degée, Ph.; Bourbigot, S.; Delobel, R.; Fontaine, G.; Devaux, E. Polylactide-based compositions. WO patent 095874 Al, 2008.
15. Technology Focus Report: Toughened PLA, NatureWorks, Ver.3/1/2007.
16. Anderson, K. S.; Schreck, K. M.; Hillmyer, M. A. Polym Rev 2008, 48, 85.
17. DuPont Biomax Strong 100 – Ethylene copolymer resin, Product Data Sheet, www.dupont.com, September 2006.
18. Flexman, E. A.; Uradnisheck, J. Toughened poly(lactic acid) compositions. US patent 7,381,772 (2008).
19. Hall, E. S.; Kolstad, J. J., Conn, R. S. E.; Gruber, P. R.; Ryan, C. M. Melt-stable lactide polymer nonwoven fabric and process for manufacture thereof. US patent 6,355,772 (2002).
20. Murariu, M.; Da Silva Ferreira, A.; Duquesne, E.; Bonnaud, L.; Dubois, Ph. Macromol Symp 2008, 272, 1.
21. Afrifah, K. A.; Matuana, L. M. Macromol Mater Eng 2010, 295, 802.
22. Degee, Ph.; Dubois, Ph.; Jerome, R. Macromol Chem Phys 1997, 198, 1985.
23. Wachsen, O.; Platkowski, K.; Reichert, K. H. Polym Degrad Stabil 1997, 57, 87.
24. Imre, B.; Renner, K.; Móczó, J.; Murariu, M.; Dubois, Ph.; Pukánszky, B. Biomacromolecules, submitted.
25. Kowalska, E.; Wielgosz, Z. J Reinf Plast Comp 2002, 21, 1013.
26. Kowalska, E.; Kawińska, B. J Reinf Plast Comp 2002, 21, 1043.
27. Zuiderduin, W. C. J.; Westzaan, C.; Huétink, J.; Gaymans, R. J. Polymer 2003, 44, 261.